First-principles description of anomalously low lattice thermal conductivity in thermoelectric Cu-Sb-Se ternary semiconductors

Yongsheng Zhang, Eric Skoug, Jeffrey Cain, Vidvuds Ozoliņš, Donald Morelli, and C. Wolverton

Phys. Rev. B **85**, 054306 — Published 21 February 2012

DOI: 10.1103/PhysRevB.85.054306

(submitted to Phys. Rev. B)

First-principles description of anomalously low lattice thermal conductivity in thermoelectric Cu-Sb-Se ternary semiconductors

Yongsheng Zhang[1], Eric Skoug[2], Jeffrey Cain[2], Vidvuds Ozoliņš[3], Donald Morelli[2], and C. Wolverton[1]

[1] *Department of Materials Science & Engineering, Northwestern University, Evanston, Illinois 60208, USA*

[2] *Department of Chemical Engineering & Materials Science, Michigan State University, East Lansing, Michigan 48824, USA*

[3] *Department of Materials Science & Engineering, University of California, Los Angeles, California 90095-1595, USA*

(Dated: February 6, 2012)

Experimental measurements have recently shown that Cu_3SbSe_3 exhibits anomalously low and nearly temperature independent lattice thermal conductivity, whereas Cu_3SbSe_4 does not exhibit this anomalous behavior. To understand this strong distinction between these two seemingly similar compounds, we perform density functional theory (DFT) calculations of the vibrational properties of these two semiconductors within the quasi-harmonic approximation. We observe strikingly different behavior in the two compounds: almost all the acoustic mode Grüneisen parameters are negative in Cu_3SbSe_4, whereas almost all are positive in Cu_3SbSe_3 throughout their respective Brillouin zones. The average of the square of the Grüneisen parameter for the acoustic mode in Cu_3SbSe_3 is larger than that of Cu_3SbSe_4, which theoretically confirms that Cu_3SbSe_3 has a stronger lattice anharmonicity than Cu_3SbSe_4. The soft frequency and high Grüneisen parameters in Cu_3SbSe_3 arise from the electrostatic repulsion between the lone s^2 pair at Sb sites and the bonding charge in Sb-Se bonds. Using our first-principles determined longitudinal and transverse acoustic mode Grüneisen parameters, zone-boundary frequencies, and phonon group velocities, we calculate the lattice thermal conductivity using the Debye-Callaway model. The theoretical thermal conductivity is good agreement with the experimental measurements.

PACS numbers: 61.50.Ah, 63.20.Ry,63.20.D-

I. INTRODUCTION

Thermoelectric materials play many promising roles in problems of energy efficiency, such as converting waste heat into power[1]. The conversion efficency is characterized by the thermoelectric figure of merit (Z): $ZT = S\sigma^2 T/\kappa$, where S is the Seebeck coefficient, σ is the electrical conductivity and κ is the thermal conductivity. Enhancing the figure of merit can be achieved by increasing S or σ, or decreasing κ. Many methodologies have been developed to improve ZT, for example enhancing Seebeck coefficients by introducing quantum confinement effects[2] and electron energy filtering[3], obtaining a high thermoelectric power factor[4–6] by producing unusual electron density of states effects, achieving a low lattice thermal conductivity in phonon-glass electron crystal compounds[7,8] and creating nanostructured materials[9,10].

Although nanostructured materials reduce thermal conductivity by enhancing phonon scattering, they also can scatter electrons, which decreases the electrical conductivity as well. A solution is to seek materials with ordered crystal structures having low thermal conductivity due to strong lattice anharmonicity, such as the ternary semiconductors $AgSbTe_2$[11] ($\kappa \sim 0.7$ $Wm^{-1}K^{-1}$ at 300 K) and Cu_3SbSe_3[12] ($\kappa \sim 0.63{-}1.0$ $Wm^{-1}K^{-1}$ at 300 K). Additionally, in Refs. 11 and 12, the authors investigated the thermal conductivity of two similar compounds: $AgInTe_2$ (which has similar stoichiometry to $AgSbTe_2$) and Cu_3SbSe_4 (which contains the same elements as Cu_3SbSe_3), and showed that $AgInTe_2$ and Cu_3SbSe_4 only exhibit classical thermal conductivity (the thermal conductivity decreases with increasing temperature).

Valence considerations based on atomic electronegativities suggest that Ag/Cu, In and Te/Se like to lose one, lose three and gain two valence electrons to form Ag^+/Cu^+, In^{3+}, and Te^{2-}/Se^{2-} ionic states, respectively. Sb, as a group-V element, can lose electrons either from the outermost p state or from p and s states, and form Sb^{3+} and Sb^{5+} valence states. In order to balance the charges in the compounds, the formal charge state of Sb should be Sb^{3+}, Sb^{5+}, and Sb^{3+} in $AgSbTe_2$, Cu_3SbSe_4, and Cu_3SbSe_3, respectively. Therefore, all valence electrons participate in the bonding in $AgInTe_2$ and Cu_3SbSe_4, while in the $AgSbTe_2$ and Cu_3SbSe_3 compounds there are two non-bonded electrons originating from the valence shell of Sb, and these non-bonding electrons play a vital role in the low lattice thermal conductivity[11,12], which was suggested by Zhuze in 1958[16].

In this paper, we focus on two Cu-Sb-Se compounds, Cu_3SbSe_4 and Cu_3SbSe_3 (Fig. 1), and theoretically study their harmonic and anharmonic vibrational properties (phonon density of states, phonon dispersion, and Grüneisen parameters) by density-functional theory (DFT) phonon calculations within the quasi-harmonic approximation. Using the Cu_3SbSe_4 and Cu_3SbSe_3 phonon dispersions, we evaluate their longitudinal acoustic (LA) and transverse acoustic (TA/TA') Grüneisen parameters ($\gamma_{\mathrm{TA/TA'/LA}}$), Debye temperatures ($\Theta_{\mathrm{TA/TA'/LA}}$), and their corresponding

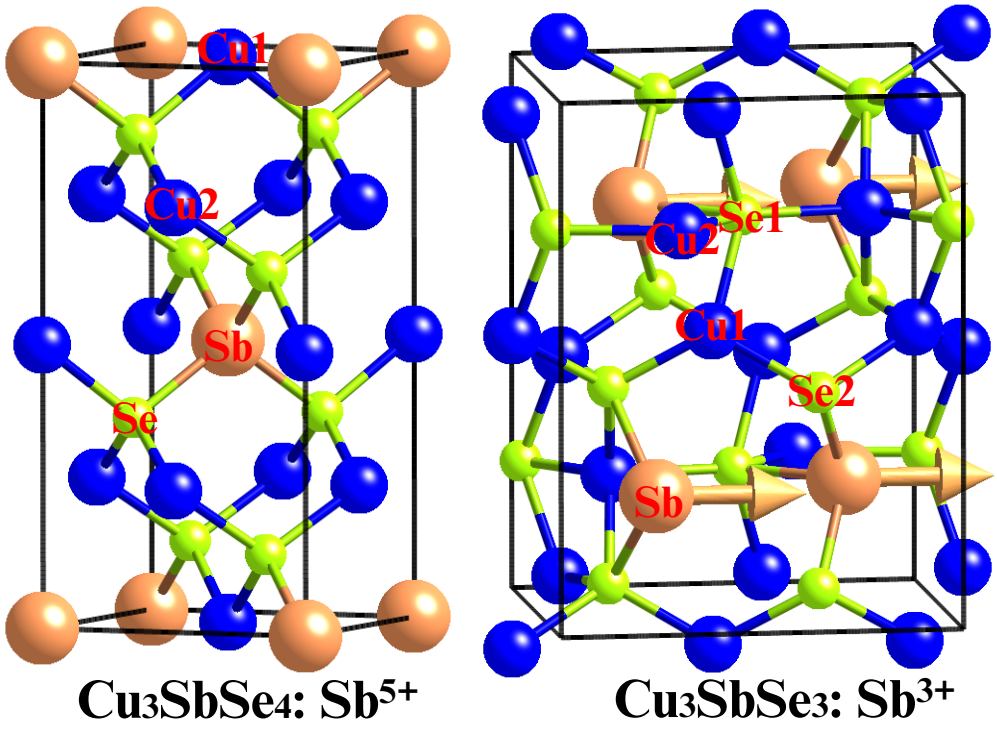

FIG. 1. (Color online) Cu_3SbSe_4[17] (the left panel): tetragonal (I42m), a^{exp}=b^{exp}=5.66 Å, c^{exp}=11.28 Å. Cu_3SbSe_3[18] (the right panel): orthorhombic (Pnma), a^{exp}=7.99 Å, b^{exp}=10.61 Å, c^{exp}=6.84 Å. The arrows on Sb atoms in Cu_3SbSe_3 represent atomic displacements responsible for the anomalously high Grüneisen parameters of the transverse acoustic phonon branch.

phonon velocities ($v_{TA/TA'/LA}$). Cu_3SbSe_3 has larger Grüneisen parameters, smaller Debye temperatures, and lower phonon velocities than Cu_3SbSe_4. Using these parameters, we calculate the lattice thermal conductivities of the two compounds from the Debye-Callaway model[28,31]. The theoretical lattice thermal conductivity is in good agreement with the experimental measurements.

II. METHODOLOGY

A. Density-functional theory and phonon calculations

We perform DFT calculations using the Vienna Ab Initio Simulation Package (VASP) code with the projector augmented wave (PAW) scheme,[19] and the generalized gradient approximation of Perdew, Burke and Ernzerhof[20] (GGA-PBE) for the electronic exchange-correlation functional. The energy cutoff for the plane wave expansion is 800 eV. We treat $3d^{10}4s^1$, $5s^25p^3$, and $2s^22p^4$ as valence electrons in Cu, Sb and Se atoms, respectively. The Brillouin zones are sampled by Monkhorst-Pack[21] k-point meshes for all compounds with meshes chosen to give a roughly

constant density of k-points (30 Å^3) for all compounds. Atomic positions and unit cell vectors are relaxed until all the forces and components of the stress tensor are below 0.01 eV/Å and 0.2 kbar, respectively. Vibrational properties are calculated using the supercell (64 and 54 atoms in Cu_3SbSe_4 and Cu_3SbSe_3 supercells, respectively) force constant method[23] by ATAT[22]. In the quasi-harmonic DFT phonon calculations, the system volume is isotropically expanded by +6% from the DFT relaxed volume.

B. Lattice thermal conductivity

Following the approach used in Refs. 28 and 29, the total thermal conductivity (κ) is written as a sum over one longitudinal ($\kappa_{\rm LA}$) and two transverse ($\kappa_{\rm TA}$ and $\kappa_{\rm TA'}$) acoustic phonon branches,

$$\kappa = \kappa_{\rm LA} + \kappa_{\rm TA} + \kappa_{\rm TA'} \quad . \tag{1}$$

These partial thermal conductivities are functions of phonon scattering rates, $1/\tau_c$, where τ_c is the relaxation time. In a solid, the total phonon scattering rate[24,25] ($1/\tau_c$) involves the contributions from normal phonon scattering ($1/\tau_N$), Umklapp phonon-phonon scattering ($1/\tau_U$), mass-difference impurity scattering ($1/\tau_m$), boundary scattering ($1/\tau_b$), and phonon-electron scattering ($1/\tau_{ph-e}$). In polycrystalline materials with low impurity concentration, such as the Cu_3SbSe_4 and Cu_3SbSe_3 samples studied in this work, the latter three phonon scattering contributions can be ignored at temperatures above approximately 100 K, since the normal and Umklapp phonon-phonon processes dominate the phonon scattering ($1/\tau_c = 1/\tau_N + 1/\tau_U$). Using the Debye-Callaway model[28,31], the partial conductivities κ_i (i corresponds to LA, TA or TA' modes) are given by,

$$\kappa_i = \frac{1}{3} C_i T^3 \{ \int_0^{\Theta_i/T} \frac{\tau_c^i(x) x^4 e^x}{(e^x-1)^2} dx + \frac{[\int_0^{\Theta_i/T} \frac{\tau_c^i(x) x^4 e^x}{\tau_N^i (e^x-1)^2} dx]^2}{\int_0^{\Theta_i/T} \frac{\tau_c^i(x) x^4 e^x}{\tau_N^i \tau_U^i (e^x-1)^2} dx} \} \quad , \tag{2}$$

where Θ_i is the longitudinal (transverse) Debye temperature,

$$x = \frac{\hbar\omega}{k_B T} \quad , \tag{3}$$

and

$$C_i = \frac{k_B^4}{2\pi^2 \hbar^3 v_i} \quad . \tag{4}$$

Here $\hbar$ is the Planck constant, k_B is the Boltzmann constant, ω is the phonon frequency, and v_i is the longitudinal or transverse acoustic phonon velocity.

For the normal phonon scattering[28,30], we can write,

$$\frac{1}{\tau_N^{\mathrm{LA}}(x)} = \frac{k_B^3 \gamma_{\mathrm{LA}}^2 V}{M\hbar^2 v_{\mathrm{LA}}^5} (\frac{k_B}{\hbar})^2 x^2 T^5 \quad , \tag{5}$$
$$\frac{1}{\tau_N^{\mathrm{TA/TA'}}(x)} = \frac{k_B^4 \gamma_{\mathrm{TA/TA'}}^2 V}{M\hbar^3 v_{\mathrm{TA/TA'}}^5} \frac{k_B}{\hbar} x T^5 \quad ,$$

and for the Umklapp phonon-phonon scattering[28,30], we can write,

$$\frac{1}{\tau_U^i(x)} = \frac{\hbar\gamma^2}{M v_i^2 \Theta_i} (\frac{k_B}{\hbar})^2 x^2 T^3 e^{-\Theta_i/3T} \quad , \tag{6}$$

where γ, V and M are the Grüneisen parameter, the volume per atom and the average mass of an atom in the crystal, respectively. From Eq. 6, we can see that the anharmonicity scattering is proportional to γ^2. Although there are several different forms[13,26,28] for the Umklapp scattering rate that differ in detail, all of them show a quadratic dependence on Grüneisen parameter. The Grüneisen parameter can be defined as[27],

$$\gamma_i = -\frac{V}{\omega_i} \frac{\partial \omega_i}{\partial V} \quad , \tag{7}$$

and it characterizes the relationship between phonon frequency and volume change.

III. CRYSTAL STRUCTURES OF Cu_3SbSe_4 AND Cu_3SbSe_3

The Cu_3SbSe_4 and Cu_3SbSe_3 crystal structures (Fig. 1) used to carry out DFT calculations are zincblende-based tetragonal (I42m)[17] and orthorhombic (Pnma)[18], which are confirmed in a recent experiment[6]. After DFT geometric relaxation, the Cu_3SbSe_4 and Cu_3SbSe_3 lattice constants are a=b=5.74 Å, c=11.40 Å and a=8.10 Å, b=10.68 Å, c=6.93 Å, respectively, which are slightly higher than the experimental data (Cu_3SbSe_4: a^{exp}=b^{exp}=5.66 Å, c^{exp}=11.28 Å; Cu_3SbSe_3: a^{exp}=7.99 Å, b^{exp}=10.61 Å, c^{exp}=6.84 Å). These DFT errors are $\sim 1-2\%$ overestimates, typical of the PBE functional. From their crystal structures (Fig. 1), in Cu_3SbSe_4 there are two inequivalent Cu atoms (Cu1 and Cu2 in the left panel of Fig. 1), and each Cu and Sb atom has four Se nearest neighbors (Cu-Se bond length: 2.43 Å and Sb-Se bond length: 2.66 Å). Cu_3SbSe_3 has a more complicated geometrical structure: there are two inequivalent Cu atoms (Cu1 and Cu2 in the right panel of Fig. 1) and two inequivalent Se atoms (Se1 and Se2 in the right panel of Fig. 1); Cu1 is neighbored by three Se (Cu-Se bond length: 2.41 Å), and one Cu (Cu-Cu bond length: 2.60 Å); Cu2 is additionally coordinated with another Cu atom; Sb has three Se neighbors (Sb-Se bond length: 2.64 Å); and Se1/Se2 is neighbored by three Cu and one Sb. This complexity in Cu_3SbSe_3 would suggest a lower thermal conductivity than that of Cu_3SbSe_4 as discussed in Refs. 13–15.

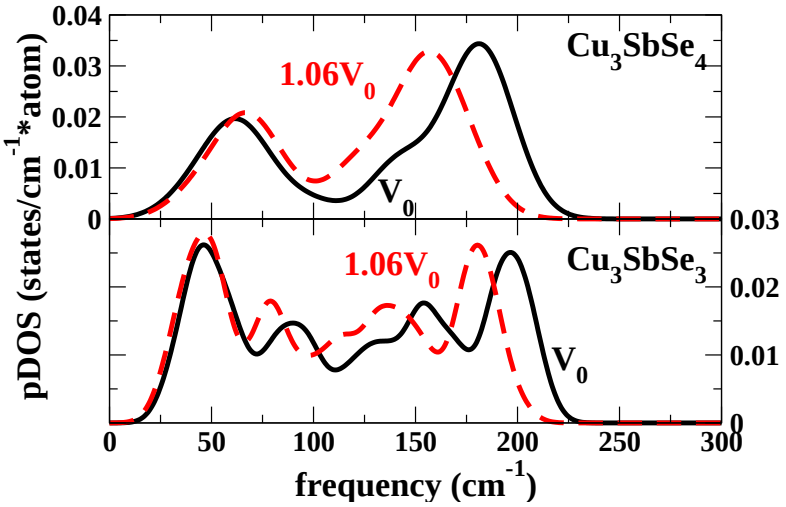

FIG. 2. (Color online) Phonon density of states (pDOS) at different volumes of Cu_3SbSe_4 (the top panel) and Cu_3SbSe_3 (the bottom panel). The black solid and red dashed lines are the pDOS at equilibrium volume (V_0) and increased volume ($1.06V_0$).

IV. ANHARMONIC VIBRATIONAL EFFECTS OF Cu_3SbSe_4 AND Cu_3SbSe_3

A. Phonon density of states

As mentioned above, Cu_3SbSe_3 has been found to exhibit strong anharmonicity and low lattice thermal conductivity, presumably arising from a strong phonon anharmonicity[12]. We have carried out phonon density of states (pDOS in Fig. 2) calculations at both the equilibrium (V_0) and increased +6% volumes ($1.06V_0$) using the supercells specified in Sec. II A. For Cu_3SbSe_3 (the bottom panel in Fig. 2), the phonon density of states shows the typical behavior of decreasing phonon frequency with increasing volume, caused by weaker interatomic bonding upon volume expansion. However, the shift in pDOS with increasing volume for Cu_3SbSe_4 (the top panel in Fig. 2) is distinct from that in Cu_3SbSe_3. The pDOS width of Cu_3SbSe_4 shrinks with increasing volume. At low frequencies (acoustic modes with ω <70 cm^{-1} in Cu_3SbSe_4 and ω <30 cm^{-1} in Cu_3SbSe_4 in Fig. 3), upon increasing the volume we find that the acoustic frequencies in Cu_3SbSe_4 (Cu_3SbSe_3) are higher (lower) than at their equilibrium volumes, respectively. Applying the Grüneisen parameter equation (Eq 7) for the acoustic modes, the average Grüneisen parameter of Cu_3SbSe_3 is positive, indicative of the typical frequency variation with volume: increasing volume softens phonon frequencies. However, for Cu_3SbSe_4 in the acoustic frequency region, the Grüneisen parameters are negative, which is a common behavior in many tetrahedral semiconductors[32], such as Si, Ge, and GaAs. For the high−frequency optical modes (ω >70 cm^{-1} in Cu_3SbSe_4 and ω >30 cm^{-1} in Cu_3SbSe_4), Cu_3SbSe_3 and Cu_3SbSe_4 show the same behavior with volume change: the optical frequencies decrease with increasing volume, and the optical Grüneisen

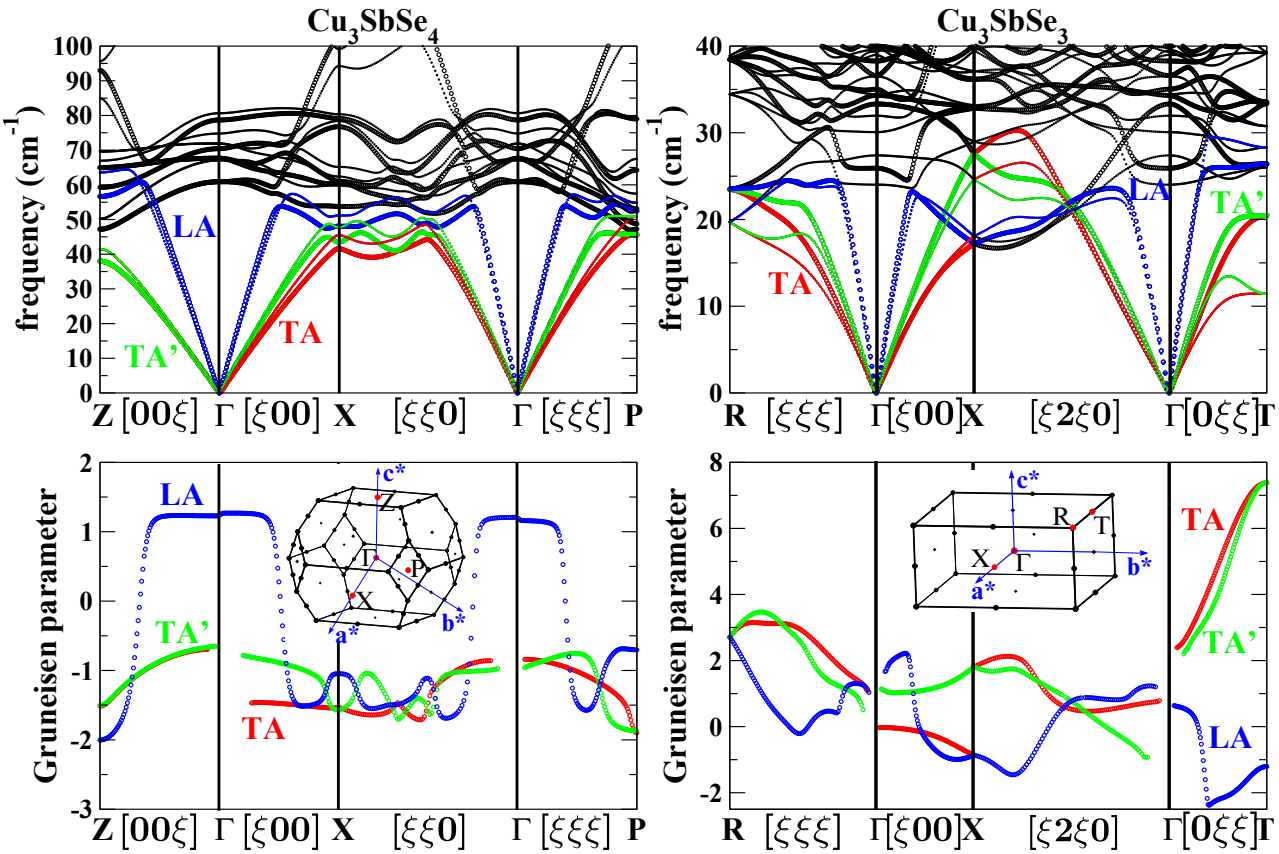

FIG. 3. (Color online) Phonon dispersions (the top panels) and corresponding acoustic Grüneisen parameters (the bottom panels) of Cu_3SbSe_4 (the left panels) and Cu_3SbSe_3 (the right panels). The big circle lines and small dotted lines in the dispersions represent the phonon dispersions at the DFT equilibrium volume and the expansion cell (+6%), respectively. The red, green and blue lines highlight TA, TA' and LA modes, respectively. The inset figures are the first Brillouin Zones of the two compounds with high symmetry points (red points) we considered in our phonon dispersion calculations.

parameters are positive for both Cu_3SbSe_3 and Cu_3SbSe_4. These results suggest that at low temperatures, where only the acoustic phonon modes are thermally excited and therefore modes with negative Grüneisen parameters dominate, thermal expansion of Cu_3SbSe_4 should be negative, whereas for Cu_3SbSe_3, where all Grüneisen parameters are positive, thermal expansion should remain positive at all temperatures.

B. Phonon dispersions

In order to get a better understanding of the anharmonic behavior of the two Cu-Sb-Se compounds, we plot the calculated phonon dispersion curves (the top panels in Fig. 3) at different volumes (V_0 and $1.06V_0$) along the high symmetry directions in their respective Brillouin Zones (BZ) (insets in Fig. 3). Since the acoustic modes play an

TABLE I. Average longitudinal (LA) and transverse (TA/TA') Grüneisen parameters ($\bar{\gamma}_{\mathrm{TA/TA'/LA}}$), Debye temperatures ($\Theta_{\mathrm{TA/TA'/LA}}$) and phonon velocities ($v_{\mathrm{TA/TA'/LA}}$) in Cu_3SbSe_4 and Cu_3SbSe_3 calculated from the phonon dispersion (Fig. 3). The Debye temperate is calculated using $\Theta = \omega_D/k_B$ (ω_D is the largest acoustic frequency in each direction); the phonon velocity is the slope of the acoustic phonon dispersion around Γ point. The Grüneisen parameters, Debye temperatures and phonon velocities are averaged by the weight of the high symmetry points.

System	$\bar{\gamma}_{\mathrm{TA}}$	$\bar{\gamma}_{\mathrm{TA'}}$	$\bar{\gamma}_{\mathrm{LA}}$	Θ_{TA} (K)	$\Theta_{\mathrm{TA'}}$ (K)	Θ_{LA} (K)	v_{TA} (m/s)	$v_{\mathrm{TA'}}$ (m/s)	v_{LA} (m/s)
Cu_3SbSe_4	1.27	1.14	1.26	60	65	78	1485	1699	3643
Cu_3SbSe_3	3.03	2.92	1.26	33	34	36	1072	1344	3014

important role in the thermal conduction, we highlight these modes with different colors in the plot. For both compounds the acoustic branches overlap with the optical modes, which leads to strong mixing and highly nonlinear dispersion curves away from center of the Brillouin zone. In Cu_3SbSe_4, avoided crossings between the longitudinal optical (LO) and longitudinal acoustic (LA) modes lead to abrupt changes in the slope of the LA phonon dispersion approximately midway to the zone boundary. Similar, but seemingly more pronounced avoided crossings can be seen in the phonon dispersion of the Cu_3SbSe_3 compound, where the LA phonon branch retains its acoustic character only within a small region of wave vectors with $|q|$ <0.2 Å^{-1}. Avoided crossings also show up in the calculated Grüneisen parameters as sharp changes in the calculated $\gamma_i(q)$, which is defined below, see the bottom panel of Fig. 3.

In contrast, the transverse acoustic branches in both compounds exhibit rather normal behavior, their frequencies smoothly rising towards the zone boundaries and saturating at approximately 40−50 cm^{-1} in Cu_3SbSe_4 and at 10−30 cm^{-1} in Cu_3SbSe_3. To compare these frequency values, we note that the dimensions of the of the unit cells of these compounds are different: the tetragonal c lattice parameter of Cu_3SbSe_4 is 7% larger than the orthorhombic b parameter of Cu_3SbSe_3, and the a lattice parameter of Cu_3SbSe_4 is approximately 40% and 20% smaller than the a and c parameters of Cu_3SbSe_3. Thus, the extent of the Brillouin zones along the Γ-Z direction in Cu_3SbSe_4 is similar to that along the Γ-T direction in Cu_3SbSe_3, and it is meaningful to compare the corresponding zone boundary frequencies. Figure 3 shows that the zone-boundary Z point TA frequency in Cu_3SbSe_4 is almost two times higher than the TA frequencies at the T point in Cu_3SbSe_3. Similarly, the LA frequencies in Cu_3SbSe_4 rise to a range of 50−60 cm^{-1}, while in Cu_3SbSe_3 the LA branch never exceeds 30 cm^{-1}. Hence, we conclude that the Cu_3SbSe_4 compound has significantly stiffer interatomic bonds and higher acoustic mode frequencies. It can be argued that

partly the softer LA phonon frequencies of Cu_3SbSe_3 can be attributed to avoided crossings with the low-lying LO branches, but this is just another manifestation of the softer interatomic bonding in this compound.

C. Grüneisen parameters

We previously discussed (Eq. 6) that the Umklapp scattering $\frac{1}{\tau_u}$ is proportional to γ^2. Thus, the Grüneisen parameters provide an estimate of the strength of the anharmonicity in a compound. Applying Eq. 7, we have calculated the dispersion of the Grüneisen parameters for all acoustic modes (the bottom panels of Fig. 3)[34]. From Fig. 3, we find that in Cu_3SbSe_4, the Grüneisen parameters are mostly negative throughout its Brillouin zone (BZ), and only in a small region around the Γ point are the Grüneisen parameters positive. But Cu_3SbSe_3 shows a different behavior, as most of the Grüneisen parameters are positive throughout the BZ.

One of the most interesting features of the phonon dispersions in Fig. 3 is the unusually high values of the Grüneisen parameter for the TA modes in Cu_3SbSe_3, particularly along the Γ-T and Γ-R directions. We see that $\gamma_{\rm TA}(q)$ rises from 3 at $q = 0$ to ∼7 at the zone boundary T point, indicating that the TA branch in Cu_3SbSe_3 is very anharmonic and interacts strongly with other acoustic phonons. Analysis of the mode eigenvectors shows that this mode involves in-phase vibrations along [100] for two out of the four Sb ions in each unit cell; the right panel in Fig. 1 schematically shows the corresponding displacement pattern. We note that the Sb lone s^2 pair charge also lies along this direction, away from the electronic charge in the three Sb-Se bonds. Intuitively, one can understand the soft frequency and high Grüneisen parameter as arising from the same physical effect: electrostatic repulsion between the lone pair and the bonding charge in Sb-Se bonds. Indeed, upon volume expansion, the Se-Sb-Se bond angle is decreased and the lone pair charge experiences stronger repulsion from the Se anions. This repulsion contributes a term to the total restoring force that acts to increase the bond angle and therefore the effective restoring force for this mode drops significantly. We conclude that first-principles DFT calculations bear out the intuitive physical picture proposed in Ref. 35, where low thermal conductivity and soft phonon frequencies were correlated with the magnitude of Se-Sb-Se bond angles.

We further calculate the average Grüneisen parameter ($\bar{\gamma}$) of each acoustic dispersion (Table I) by the method described in Ref. 28: $\bar{\gamma} = \sqrt{<\gamma_i^2>}$. In Cu_3SbSe_4, $\bar{\gamma}_{\rm TA}$, $\bar{\gamma}_{\rm TA'}$ and $\bar{\gamma}_{\rm LA}$ are nearly identical, and average of the three acoustic Grüneisen parameters is $\bar{\gamma}_A$ =1.22. This value is close to the Grüneisen parameter of PbTe (γ ≈1.45)[13], which has a relatively high value of lattice thermal conductivity (2.4 W m^{-1}K^{-1} at 300 K)[11]. This can be contrasted with Cu_3SbSe_3, where the average of all three acoustic Grüneisen parameters ($\bar{\gamma}_A$=2.41) is close to that of $AgSbTe_2$ (γ ≈2.05, a low thermal conductivity material, 0.7 Wm^{-1}K^{-1} at 300 K)[11]. This similarity between the Grüneisen

parameters in Cu_3SbSe_3 and $AgSbTe_2$ is likely due to Sb having the same nominal valence state (Sb^{3+}) in both compounds, and suggests the two additional non-bonding electrons in the valence shell of Sb^{3+} play similar roles in the two compounds[11,12]. Although the longitudinal $\bar{\gamma}_{\mathrm{LA}}$ in Cu_3SbSe_3 is similar to $\bar{\gamma}_{\mathrm{LA}}$ in Cu_3SbSe_4, the transverse $\bar{\gamma}_{\mathrm{TA/TA'}}$ are much larger in Cu_3SbSe_3 than the corresponding acoustic modes in Cu_3SbSe_4. This indicates that Cu_3SbSe_3 has stronger anharmonicity and larger lattice resistance than Cu_3SbSe_4, which induces stronger Umklapp phonon scattering and lower thermal conductivity in Cu_3SbSe_3. Moreover, the transverse modes of Cu_3SbSe_3 have much larger Grüneisen parameters than the longitudinal mode, and these transverse modes play an important role in lattice thermal resistance. Lattice thermal conductivity tends to be dominated by the lower velocity transverse modes[33].

D. Thermal conductivity

Using the phonon dispersions (Fig. 3), we can further evaluate the longitudinal (LA) and transverse (TA/TA') Debye temperatures ($\Theta_{\mathrm{TA/TA'/LA}}$) and their corresponding phonon velocities ($v_{\mathrm{TA/TA'/LA}}$) in Cu_3SbSe_4 and Cu_3SbSe_3 (Table I). In Ref. 12, the authors used a Debye temperature of 131 K for Cu_3SbSe_4 in the Slack model[13], which is larger than our theoretical calculation (Table I). Moreover, for Cu_3SbSe_3, the authors[12] estimated the minimum thermal conductivity by $\kappa = C_v v L/3$ using $v = 3000$ m/s, and stated that the phonon velocity is a reasonable value for a solid. However, from our theoretical calculations, we find that only the longitudinal phonon velocity is close to 3000 m/s; the transverse phonon velocities are much smaller than 3000 m/s.

Inserting our DFT calculated quantities (Table I) in Eq. 1 and Eq. 2, we can calculate the lattice thermal conductivities of the two compounds with no adjustable parameters (Fig. 4). From Fig. 4, we can see a good agreement between our theoretical calculations and experimental measurements. The diamond-like Cu_3SbSe_4 (the black solid line in Fig. 4) exhibits classical behavior (the thermal conductivity is decreasing with increasing temperature roughly as T^{-1}), while the lattice thermal conductivity in Cu_3SbSe_3 (the red solid line in Fig. 4) is anomalously low and nearly temperature independent. The deviation between the experimental data and the calculated curves might be because that the Debye-Callaway model does not take into account optical modes, which happen to be quite low in the two Cu-Sb-Se compounds and that some of them have appreciable group velocities. But the deviation for both cases is at most only about 20%, which is quite satisfactory given the approximations inherent in the Debye-Callaway formalism. We conclude that the near-intrinsically minimal lattice thermal conductivity of Cu_3SbSe_3 arises due to the combination of a very low Debye temperature, and a large average Grüneisen parameter in this compound (Table

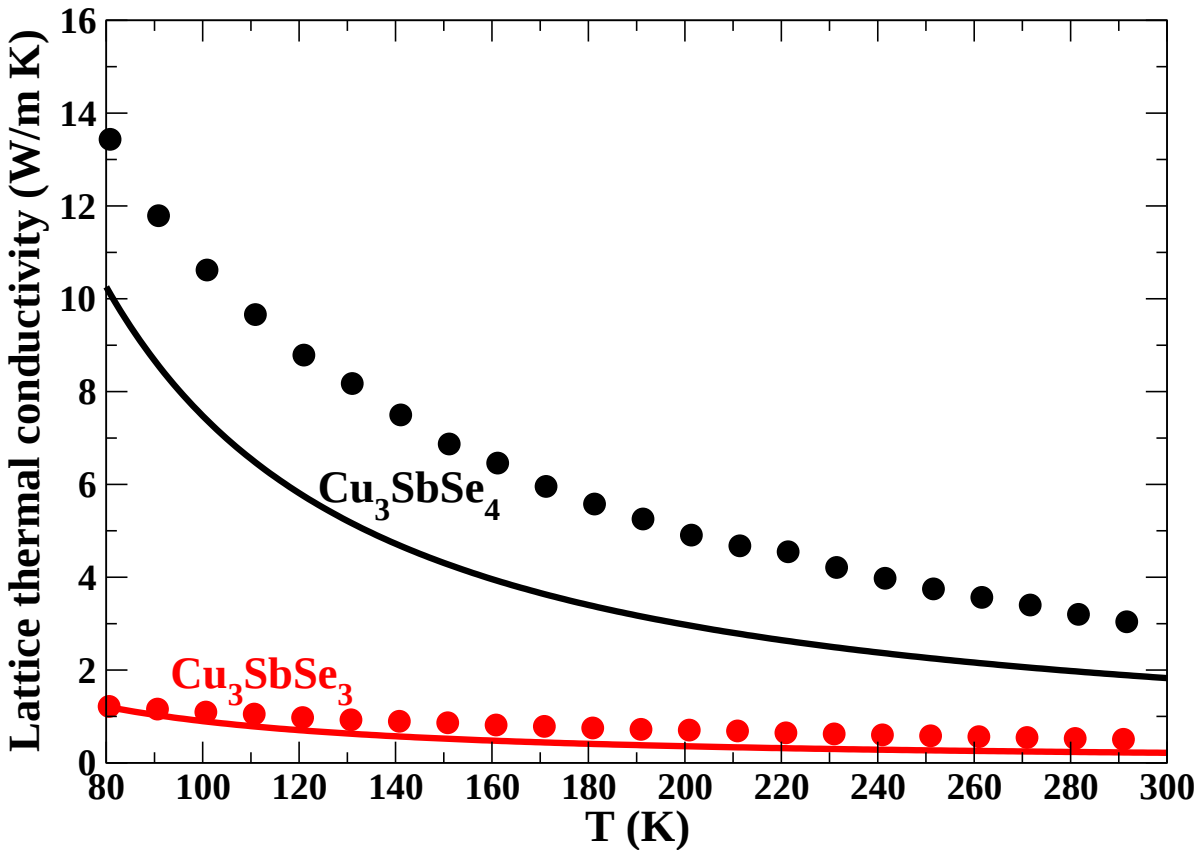

FIG. 4. (Color online) Lattice thermal conductivity of Cu_3SbSe_4 and Cu_3SbSe_3. The black and red filled circles are experimental measurements (from Ref. 12) of Cu_3SbSe_4 and Cu_3SbSe_3, respectively. The black and red solid lines represent the theoretical thermal conductivity of Cu_3SbSe_4 and Cu_3SbSe_3 using their corresponding Grüneisen parameters (γ), Debye temperatures (Θ) and phonon velocities (v) in Table I.

I).

V. SUMMARY

Two Cu-Sb-Se semiconductors, Cu_3SbSe_4 and Cu_3SbSe_3, have been studied by DFT calculations. We perform DFT phonon calculations with the quasi-harmonic approximation, and compute the Grüneisen parameters of the two compounds. The Grüneisen parameters for the acoustic modes are mostly negative in Cu_3SbSe_4, and mostly positive in Cu_3SbSe_3 throughout their respective BZ. Based on average Grüneisen parameters, we suggest that Cu_3SbSe_3 has stronger anharmonicity and larger lattice resistance than Cu_3SbSe_4. The transverse acoustic modes, which are particularly important for lattice heat conduction, also have a larger contribution to the anharmonicity than the longitudinal mode. The soft frequency and high Grüneisen parameters in Cu_3SbSe_3 arise from the electrostatic

repulsion between the lone s^2 pair at Sb sites and the bonding charge in Sb-Se bonds. Using our theoretically determined longitudinal (LA) and transverse (TA/TA') Grüneisen parameters, Debye temperatures ($\Theta_{\mathrm{TA/TA'/LA}}$) and their corresponding phonon velocities ($v_{\mathrm{TA/TA'/LA}}$), we calculate the lattice thermal conductivity by the Debye-Callaway model. We find a good agreement between the theoretical calculations and the experimental measurements.

ACKNOWLEDGMENTS

Collaborative work among NU, MSU and UCLA is supported as part of the Center for Revolutionary Materials for Solid State Energy Conversion, an Energy Frontier Research Center funded by the U.S. Department of Energy, Office of Science, Office of Basic Energy Sciences under Award Number DE-SC0001054.

[1] L. E. Bell, Science **321**, 1457 (2008).

[2] T. C. Harman, P. J. Taylor, M. P. Walsh and B. E. LaForge, Science **297**, 2229 (2002).

[3] J. P. Heremans, C. M. Thrush and D. T. Morelli, Phys. Rev. B **70**, 115334 (2004).

[4] D. M. Rowe, G. Min and V. L. Kuznestov, Phil. Mag. Let. **77**, 105 (1998).

[5] M. Vasundhara, V. Srinivas and V. V. Rao, J. Phys. Condensed Matter **17**, 6025 (2005).

[6] E. J. Skoug, C. Zhou, Y. Pei and D. T. Morelli, Appl. Phys. Lett. **94**, 022115 (2009).

[7] D. T. Morelli and G. P. Meisner, Jour. Appl. Phys. **77**, 3777 (1995).

[8] G. S. Nolas, J. L. Cohn, G. A. Slack and S. B. Shujman, Appl. Phys. Lett. **73** 178 (1998).

[9] K. F. Hsu, S. Loo, F. Guo, W. Chen, J. S. Dyck, C. Uher, T. Hogan, E. K. Polychroniadis and M. G. Kanazidis, Science **303**, 818 (2004).

[10] B. Poudel, Q. Hao, Y. Ma, Y. Lan, A. Minnich, B. Yu, X. Yan, D. Wang, A. Muto, D. Vashaee, X. Chen, J. Liu, M. S. Dresselhaus, G. Chen and Z. Ren, Science **320**, 634 (2008).

[11] D. T. Morelli, V. Jovovic and J. P. Heremans, Phys. Rev. Lett. **101**, 035901 (2008).

[12] E. J. Skoug, J. D. Cain and D. T. Morelli, Appl. Phys. Lett. **96**, 181905 (2010).

[13] G. A. Slack, Solid State Physics, **34**, 1 (1979).

[14] A. Zevalkink, E. S. Toberer, W. G. Zeier, E. Flage-Larsen and G. J. Snyder, Energy Environ. Sci. **4**, 510 (2011).

[15] E. S. Toberer, A. F. May and G. J. Snyder, Chem. Mater. **22**, 624 (2009).

[16] V. P. Zhuze, V. M. Shtrum, Sov. Phys. Tech. Phys. **3**, 1925 (1958).

[17] J. Garin and E. Parthé, Acta Cryst. **B28**, 3672 (1972).

[18] A. Pfitzner, Zeit. Kristall. **209**, 685 (1994).

[19] G. Kresse and D. Joubert, Phys. Rev. B **59**, 1758 (1999).

[20] J. P. Perdew, K. Burke, and M. Ernzerhof, Phys. Rev. Lett. **77**, 3865 (1996).

[21] H. J. Monkhorst and J. D. Pack, Phys. Rev. B **13**, 5188 (1976).

[22] A. Van de Walle, M. Asta and G. Ceder, CALPHAD **26**, 539 (2002).

[23] A. Van de Walle and G. Ceder, Rev. Mod. Phys. **74**, 11 (2002).

[24] G. Grimvall, *Thermophysical properties of materials*, Elsevier, (1986).

[25] J. Zou and A. Balandin, J. App. Phys. **89**, 2932 (2001).

[26] C. L. Julian, Phys. Rev. **137**, A128 (1965).

[27] M. T. Dove *Structure and Dynamics*, Oxford, (2003).

[28] D. T. Morelli, J. P. Heremans and G. A. Slack, Phys. Rev. B **66**, 195304 (2002).

[29] M. Asen-Palmer, K. Bartkowski, E. Gmelin, M. Cardona, A. P. Zhernov, A. V. Inyushkin, A. Taldenkov, V. I. Ozhogin, K. M. Itoch and E. E. Haller, Phys. Rev. B **56**, 9431 (1997).

[30] G. A. Slack and S. Galginaitis, Phys. Rev. **133**, A253 (1964)

[31] J. Callaway, Phys. Rev. **113**, 1046 (1959).

[32] C. H. Xu, C. Z. Wang, C. T. Chan and K. M. Ho, Phys. Rev. B **43**, 5024 (1991).

[33] R. Berman, *Thermal conduction in solids*, Clarendon Press, Oxford, (1976).

[34] It should be noticed that using Eq. 7 to get the acoustic Grüneisen parameters is questionable at $q \to 0$, as the Grüneisen parameter will become discontinuous as $\omega \to 0$. In Fig. 3, we simply ignore this discontinuous region around the Γ point. For some Grüneisen dispersions around Γ, the blank areas are slightly large because the numerical errors in the calculations induce a large discontinuity area. This omission will not affect our ability to detect the positive or negative Grüneisen regions and the average Grüneisen parameter of each mode in the later discussions.

[35] E. J. Skoug and D. T. Morelli, Phys. Rev. Lett. **107**, 235901 (2011).